Two-Dimensional Electron Gas ("2DEG") Hot-Electron Mixers For Millimeter Waves and Submillimeter Waves

J.-X. Yang, W. Grammer, F. Agahi, K.-M. Lau, and K.S. Yngvesson

Abstract

The lowest noise temperature for any receiver in the 0.5 to 1 THz range has been achieved with the *InSb* hot electron mixers, which unfortunately suffer from the problem of having a very narrow (1–2 MHz) bandwidth. We are investigating two–dimensional electron gas (2DEG) devices as hot electron detectors and mixers in order to circumvent this problem. High–quality heterojunction material has been grown in–house with OM-CVD, and devices fabricated with dimensions in the range 10–100 micrometers. We have designed and tested a 35 GHz mixer, operating at 77K, which has demonstrated a bandwidth of at least 2 GHz. We are also working on a 94 GHz mixer for 4.2K operation. The theory of 2DEG hot electron mixers, and their potential for low–noise receivers in the THz range are discussed.

This work was supported by the National Aeronautics and Space Administration, under grant NAGW–1659

The authors are with the Department of Electrical and Computer Engineering, University of Massachusetts, Amherst, MA 01003.

I. INTRODUCTION

Receivers at frequencies close to 1 THz have equivalent noise temperatures which are from one to two orders of magnitude higher than the ultimate limit for the noise temperature of a coherent receiver - the quantum noise limit, see Figure 1. The frequency-dependence of the noise temperature of cooled Schottky-barrier and SIS mixers is also quite steep, as seen in this figure. The lowest noise temperature in this frequency range has been demonstrated with the $InSb$ hot-electron mixer [1], which is a bulk device, and therefore has very small parasitic reactances. It is noteworthy that the frequency-dependence of the noise temperature of the $InSb$ mixer is less steep – presumably this can be explained in general terms by the low reactance of the device. In contrast, Schottky-barrier and SIS devices for this frequency range have to be fabricated with extremely small dimensions in order to minimize their reactance (primarily capacitive). The main disadvantage of the $InSb$ mixer is its very narrow bandwidth (at most a few MHz), which has limited its application in practical systems. A natural question to ask is then: Are there bulk-type devices which will result in a wider bandwidth? A paper by Smith et al. [2] proposed a two-dimensional electron gas device, operating at liquid helium temperature, and demonstrated photoconductive detection at 100 and 200 GHz, as well as at 119 micrometer wavelength. This device is essentially constructed as a fairly large HFET (heterojunction FET, also known as HEMT), without the gate. The structure of the device is shown in Figure 2. It makes use of a two–dimensional "sheet" of electrons (the two-dimensional electron gas, or "2DEG"), streaming from what would be the source of the HFET, to the drain, i.e. it is the two-dimensional analogue of the bulk $InSb$ device.

The two-dimensional geometry results in many of the same advantages, which derive from the three-dimensional geometry of the $InSb$ mixer, with a few differences which we will explore below. Most importantly, however, the bandwidth is predicted to be in the GHz range, which is sufficient for most THz applications.

We have proposed new versions of the 2DEG hot electron mixer [3], in particular we will present measured data for a 2DEG mixer, which operates at 77K. This mixer demonstrates the wide bandwidth of the 2DEG type of mixer for the first time. The paper first discusses the basic features and theory of 2DEG hot-electron detectors and mixers,

with emphasis on the latter. We then describe designs for mixers at 35 and 94 GHz, respectively, and the data obtained so far.

II. THEORY OF HOT-ELECTRON DETECTORS AND MIXERS

A. *Basic Nonlinear Mechanism*

The nonlinear mechanism behind hot electron detectors and mixers is substantially different from that of Schottky barrier and SIS mixers. In the latter, the currents at the RF and LO frequencies basically follow the I–V–curve, which can be measured at DC. The hot electron device, on the other hand, responds to the power at the RF or LO frequency, not the instantaneous voltage. This power heats the electron gas above the lattice temperature, and as a result the resistance of the device changes. The change in resistance with electron temperature can come about because of a change in electron mobility, or electron density, or a combination of these. A typical curve of resistance versus dissipated power, derived from measured data on one of our devices at 77K, is shown in Figure 3. Note that in this particular case, the slope of the curve is approximately constant, i.e.

$$R_B = C \times P \tag{1}$$

If both RF and LO power are coupled to the device, then the resistance will vary in response to the total instantaneous power as shown in Figure 4, provided that the IF frequency (f_{IF}) is such that

$$f_{IF} < \frac{1}{2\pi\tau_e} \tag{2}$$

The energy relaxation time, τ_e, determines the rate at which the average energy of the electron gas (at least approximately given by the "electron temperature") can change in response to the dissipated power imposed. If (2) is fulfilled, we will thus find that the resistance varies at the IF frequency. Given a constant current bias source, a voltage will then be developed across the load at the IF frequency, R_L, in the equivalent circuit of Figure 5. This circuit will enable us to calculate the responsivity of the device as a detector, and the conversion loss as a mixer. The useable bandwidth extends from DC to the frequency given by (2). It may be of interest to point out that the theory of hot electron mixers safely can ignore any higher order LO harmonics or sidebands.

The value of τ_e for $InSb$ in the liquid helium temperature range is about 2×10^{-7} sec, resulting in a bandwidth of about 1–2 MHz. The energy relaxation time of the 2DEG in heterostructures has been the subject of fairly intensive study, over the temperature range from 4K through 300K. In the lower temperature range, Sakai et al. [4] measured values between 10^{-10} and 10^{-9} seconds, indicating that bandwidths of about 1 GHz are attainable. Shah [5] has summarized work related to the energy loss rate of the 2DEG at higher temperatures, from 50K to 150K. Values for τ_e of 10^{-11} to 10^{-10} seconds have been obtained, which indicate bandwidths of a 2DEG mixer in this temperature range up to 10 GHz.

B. *Calculation of the Conversion Loss*

Expressions for the conversion loss of hot electron mixers were given by Arams et al. [6]. These are based on the equivalent circuit in Figure 5. The conversion loss must be optimized with respect to the value of several parameters in this circuit. It is assumed that the DC power (P_{DC}) and the LO power (P_{LO}) have the same effect on the device resistance. Reference [6] derives the optimum ratio of P_{DC}/P_{LO}, for which the conversion loss is minimized, under the constraint that the total dissipated power, P_O, is constant. We also introduce $R_{BO} = V/I$, which is the equivalent device RF resistance at an operating point for which the total power dissipated is P_O. The following expression can then be obtained for the conversion loss:

$$L_c = 8\left(\frac{R_{BO}}{CP_O}\right)^2 \left[\frac{(R_L + R_{BO})^2}{4R_L R_{BO}}\right] \left[1 - \frac{CP_O}{R_{BO}}\left(\frac{R_L - R_{BO}}{R_L + R_{BO}}\right)\right] \left[1 - \left(\frac{R_{BO} - Z_O}{R_{BO} + Z_O}\right)^2\right] \left[1 + (\omega_{IF}\tau_e)^2\right] \tag{3}$$

The optimum DC power and the optimum load resistance are found from:

$$(P_{DC})_{opt} = \frac{P_O}{2 - \frac{CP_O}{R_{BO}}\left(\frac{R_L - R_{BO}}{R_L + R_{BO}}\right)} \tag{4}$$

$$(R_L)_{opt} = R_{BO}\sqrt{\frac{1 + \frac{CP_O}{R_{BO}}}{1 - \frac{CP_O}{R_{BO}}}} \tag{5}$$

We can thus calculate L_c from (3), and plot it as a function of P_{LO} by using $P_O = P_{DC} + P_{LO}$, as well as (4), given representative values for the RF circuit impedance Z_O (100 ohms), and $R_L = 50$ ohms. Figure 6 shows the measured I-V-curve for the 77K device which will be described later*). The conversion loss calculated from this curve is given in Figure 7. For convenience, an analytical fit to the I-V-curve was used, given by:

$$I = \left(\frac{2I_O}{\pi}\right) \tan^{-1}(\alpha V) \tag{6}$$

Experimental LO power was in the range of 1-4 mW, and the predicted conversion loss thus is of the order of 15–20 dB. Other devices fabricated from wafers which have been grown in-house have shown greater nonlinearity. By using these data, and assuming reasonable changes in the device dimensions, we have estimated that we can expect to improve the I-V-curve considerably. On the basis of the improved I-V-curve, we predict a considerably lower conversion loss of close to 8 dB, see Figure 8. The ultimate theoretical limit for the conversion loss is 6 dB [6]. We also calculated L_C for $InSb$, based on an I–V–curve from [1], and obtained an optimum value of about 12 dB, which is consistent with published data for this material.

C. *Variation of Device Resistance with Device Dimensions*

One of the advantages of using the two-dimensional device geometry is that it allows a great deal of flexibility for choosing the device dimensions, in order to match the requirements for an optimum detector or mixer. Its surface resistance is found from:

$$\rho_s = \frac{1}{eN_s\mu} \text{ ohms/} \square \tag{7}$$

where e is the electron charge, N_s is the electron density (cm^{-2}), and μ is the mobility. The device resistance is found by multiplying (7) by L/W, where L is the length, and W the width of the device. According to (7), devices with the same L/W can be fabricated with different areas, while maintaining the same resistance, which may be matched to a particular microwave circuit. For typical materials, ρ_s is conveniently close to the

* This device was fabricated on MBE material, courtesy of Dr. D. Masse' of Raytheon Company

impedance of microwave integrated transmission lines. For example, if $N_s = 10^{12}$ cm^{-2}, and $\mu = 63{,}000$ cm^2/Vs, $\rho_s = 100$ ohms.

Briefly, by using (3), we find that mixer devices are optimized if the initial (linear) resistance is small, while the RF and LO impedances are matched to R_{BO} at the operating point. The optimum IF impedance is 2–4 times higher than the RF impedance. The LO power required should scale with the area of the device, since the energy loss rate per electron is constant for a given electron temperature [4]. Optimum detectors should also be RF matched to R_{BO}, and the responsivity is predicted to increase with decreased area.

D. *Equivalent Circuit, Including Parasitics*

So far we assumed that the device equivalent circuit was purely resistive. In order to assess the potential of the device for THz applications, we must calculate the parasitic elements in the circuit, however. An important effect to take into account is the electron inertia which is related to the finite momentum relaxation time, τ_m [7,8].

The value of τ_m is found from the mobility as follows:

$$\tau_m = \frac{\mu m^*}{e} \tag{8}$$

As demonstrated in [7], the equivalent circuit at very high frequencies is as shown in Figure 9a. The impedance (Z_s) of the series portion of the circuit is

$$Z_s = \rho_s \times \frac{L}{W}(1 + j\omega\tau_m) = R_B + j\omega L_B = R_O(1 + j\omega\tau_m) \tag{9}$$

in terms of the low-frequency resistance, R_0. C_0 is the (frequency–independent) capacitance. The configuration of the device makes it easy to minimize C_0, in which case it is sufficiently accurate to use only Z_s for the equivalent circuit. The inductive part of Z_s becomes appreciable at a frequency for which $2\pi \times f \times \tau_m = 1$. Let's define this frequency as f_m. For typical room temperature mobilities, (8) and (9) predict that f_m is from 0.5 to 1 THz, and these phenomena are consequently not important in devices below the THz range**).

** Carrier inertia phenomena have very noticeable effects in THz harmonic multipliers, see the paper at this conference by E.L. Kollberg, T. Tolmunen, M. Frerking, and J. East, "Current Saturation in Submillimeter Wave Varactors".

At lower temperatures, however, τ_m is longer, and significant effects can be seen at frequencies of tens of GHz. At 77K, for example, a typical μ for our materials is 100,000 cm^2/Vs, and $f_m = 42$ GHz. As LO and DC power is applied, the electron temperature rises, and f_m increases as well, since τ_m becomes shorter at the higher T_e's. This effect will have to be taken into account in the mixer design. It is also not clear how good the model is, which assumes a specific value for τ_m, although it has been shown to work well in some cases for which Monte Carlo simulation was used for comparison [8]. Since f_m is as low as 30–40 GHz, it is possible to measure the equivalent circuit, however, as described below.

The reactive nature of the response of the electrons has been shown to give rise to a decrease of the responsivity of $InSb$ detectors with increasing frequency, starting at about 200–300 GHz [1]. One can circumvent this limitation by applying a small magnetic field, tuning the electrons to the cyclotron resonance. As a result, the responsivity (and the conversion loss of a mixer) becomes essentially independent of frequency up to about 2 THz. The experiment of Smith et al. [2], showed that the 2DEG device also acts as a detector at the cyclotron resonance. There are thus two conceivable methods for obtaining good response for 2DEG devices up to THz frequencies:

(1) Make use of the cyclotron resonance for enhancement. This should be feasible for devices at 4K, as well as at 77K.

(2) Add a capacitance in series, in order to tune out the 2DEG inductive reactance, as shown in the circuit model of Figure 9b.

We are planning to try both of these approaches.

E. *Noise Properties*

As shown in [6], the DSB noise temperature of a hot electron mixer receiver is approximately:

$$T_{RX} = L_c \times (T_e + T_{IF}) \tag{10}$$

Here, T_e is the electron temperature, and it is assumed that the electrons radiate thermal noise at this temperature. Shot noise has been neglected, and T_{IF} is the noise temperature of the IF amplifier, which is assumed to be matched to the mixer. For a mixer operating

at a physical temperature of 77K, T_e may be about 150K. If T_{IF} is 10K, and $L_c = 10$ dB, we find $T_{RX} = 1600$K. From the noise temperature point of view, it is clearly desirable to operate the mixer at as low a temperature as possible. For example, a 4.2K device might have $T_e = 10$ K, and $T_{RX} = 200$K for the same L_c and T_{IF}.

III. MATERIALS GROWTH AND FABRICATION OF DEVICES

The 2-DEG structures were grown by low pressure organometallic chemical vapor deposition (OMCVD) on undoped semi-insulating *GaAs* (100) substrates oriented 2° off towards the (110) planes. The sources used were trimethylaluminum, trimethylgallium, 100% arsine, and silane as n-type dopant. A typical device structure includes a 1μm *GaAs* buffer, a 100Å undoped *AlGaAs* spacer, a 500Å uniformly doped *AlGaAs*, and a 200Å doped GaAs contact layer. The *Al* content in the *AlGaAs* layers was between 29 and 33%. The dopant concentration in the doped *AlGaAs* was in the high 10^{17} to 1×10^{18} range. The reaction chamber pressure was kept at 50 torr and the growth temperature was at 700°C. A V/III ratio of > 200 was used for the growth of the *AlGaAs* layers. The thicknesses of the thin layers were nominal thicknesses determined by the growth of thick calibration layers. Hall measurements were made on the as-grown layers using the van der Pauw technique at room, liquid nitrogen, and liquid helium temperatures. The best sample obtained thus far has a sheet charge density (N_s) of 1×10^{12}/cm^2 and a 77K mobility (μ_{77}) of 95,000 cm^2/V-s. At 4.2K these values were 1×10^{12}/cm^2 and 166,000 cm^2/V-s. A carefully calibrated slow etchant was used to remove materials from the surface between 77K measurements. There were no noticeable changes in the measurements as the surface doped layers were being step-etched, indicating that there was minimal conduction in these layers competing with the 2-DEG. A standard Hall bar was fabricated on a sample piece for drift mobility and Shubnikov-de Haas measurements. Shown in Fig. 10 is the low field (mV/cm) drift mobility measured at 4.2K, which agrees well with the Hall mobility. Very strong Shubnikov-de Haas oscillations of the magnetoresistance and quantum Hall effects were observed (Fig. 11).

A double channel structure consisting of a 1μm *GaAs* buffer, a 500Å undoped *AlGaAs* buffer, a 500Å doped *AlGaAs*, a 100Å undoped *AlGaAs* spacer, a 1000Å undoped *GaAs*, a 100Å undoped *AlGaAs* spacer, and doped cap layers of *AlGaAs* and *GaAs* was also

grown. Two 2-DEG channels are formed at the top and bottom of the 1000Å *GaAs* layer. This structure has resulted in an $N_s = 2 \times 10^{12}/\text{cm}^2$ with $\mu_{77} = 64{,}400\text{cm}^2/\text{V-s}$. The $N_s\mu$ product is very high compared with any MODFET structures made with any material systems.

We believe the high sheet charge densities from the relatively low doped *AlGaAs* ($10^{17}/\text{cm}^3$ range) are a result of the high quality of the *AlGaAs* layers and interfaces, leading to very efficient transfer of electrons to the 2-DEG channels.

IV. MIXER CIRCUIT DESIGN AND EXPERIMENTAL RESULTS

A. *A 35 GHz Mixer for 77K Operation*

We plan to use the 2DEG devices with Tapered Slot Antennas (TSAs) or arrays, which makes it convenient to couple experimental mixer designs from a waveguide/finline transition inside a split block. The device is inserted across a slot-line, just outside the split block, by using a flip-chip technique, see Figure 12. The circuit is fabricated on a high-resistivity silicon substrate, 0.33 mm thick, see Figure 13. A slot-line/coplanar waveguide (CPW) transition is placed $3/4\lambda$ from the device, with a quarter-wave open CPW stub $\lambda/4$ from the transition, serving as an RF matching element and low-pass filter for the IF (1 GHz). We have chosen to use the combination of slot-line/CPW transmission lines, for the convenience of being able to produce circuits on a single side of the substrate. Wire bonds are used at all CPW discontinuities to keep ground currents in phase. A monolithic version of the mixer will use air bridges and an integrated IF amplifier, and be fabricated on a semi-insulating *GaAs* substrate.

The uniplanar silicon circuits are being developed and tested by probing them with a Cascade Microprobe. Many different configurations can be tested on a single chip, see Figure 14. We also plan to measure devices at liquid nitrogen temperature in order to derive the equivalent circuit of the device (compare the discussion in section III.D.).

The mixers are being tested in a simple cryogenic setup, which cools them to liquid nitrogen temperature. Figure 15 gives the measured onversion loss, versus frequency, for two different bias voltages. The conversion loss becomes very large for zero DC bias, as it should (see (3)). The measured conversion loss also was essentially unchanged as the IF frequency was changed between 1 and 2 GHz, a behavior which is expected since $\frac{1}{(2\pi \times \tau_e)}$

is estimated to be about 10 GHz. The conversion loss is about 10 dB higher than the theoretical prediction from Figure 7. The discrepancy in this initial experiment appears to be a circuit effect, based on the evidence that the return loss for both RF and IF is better than 10 dB, while variation of the bias has only a very small effect on the return loss. On the other hand, the conversion loss behaves as predicted when the bias and LO power are varied. Further circuit studies are expected to solve this problem.

B. *A 94 GHz Mixer for 4.2K Operation*

A similar circuit to that described above is being used to implement a 94 GHz mixer. The initial experiments are being performed to detect the cyclotron resonance in the 2DEG, and confirm the results of [2]. So far, these have been unsuccessful, but the initial device (from the same batch as the one used in the 35 GHz mixer) had a much too small impedance (about 10 ohms) when used as a detector device and was not well matched to the slotline. New devices are under fabrication, which will have closer to optimum parameters.

V. CONCLUSION

The challenge of this work is to duplicate the excellent noise temperatures achieved by *InSb* hot electron mixers in the frequency range 0.5–1 THz, while providing a much wide bandwidth, in a 2DEG device. So far, our first device has demonstrated a wide bandwidth (at least 2 GHz), while operating at 77K. Further circuit work is expected to bring the conversion loss of this mixer down to values close to those predicted by theory (about 10 dB or less). Noise temperature measurements on this mixer will enable us to establish a theoretical framework for the noise performance. The experiments by Smith et al. [2] indicate that a 4.2K device is also feasible. For a device cooled to this temperature, we can expect the noise temperature to be as low as that of the *InSb* mixer.

REFERENCES

[1] Brown, E.R., Keene, J., and Phillips, T.G., "A Heterodyne Receiver for the Submillimeter Wavelength Region Based on Cyclotron Resonance in *InSb* at Low Temperature," *Intern. J. Infrared and Millimeter Waves*, 6, 1121 (1985).

[2] Smith, S.M., Cronin, N.J., Nicholas, R.J., Brummel, M.A., Harris, J.J., and Foxon, C.T., "Millimeter and Submillimeter Detection Using $Ga_{1-x}Al_xAs/GaAs$ Heterostructures," *Intern. J. Infrared and Millimeter Waves*, 8, 793 (1987).

[3] Yang, J.-X., Grammer, W., Agahi, F., K.-M. Lau and K.S. Yngvesson, "High Mobility Hot Electron Mixers for Millimeter Waves and Submillimeter Waves," *Fifteenth Intern. Conf. Infrared and Millimeter Waves*, Orlando, FLA, Dec. 1990 (Digest), p. 248.

[4] Sakaki, H. Hirakawa, K., Yoshino, J., Svensson, S.P., Sekiguchi, Y., Hotta, T., and Nishii, S., "Effects of Electron Heating on the Two–Dimensional Magnetotransport in *AlGaAs/GaAs* Heterostructures," *Surface Science*, 142, 306 (1984).

[5] Shah, J., "Hot Carriers in Quasi-2-D Polar Semiconductors," *IEEE J. Qu. Electronics*, QE–22, 1728 (1986).

[6] Arams, F., Allen, C., Peyton, B., and Sard, E., "Millimeter Mixing and Detection in Bulk *InSb*," *Proc. IEEE*, 54, 612 (1966).

[7] Champlin, K.S., Armstrong, D.B., and Gunderson, P.D., "Charge Carrier Inertia in Semiconductors," *Proc. IEEE*, 52, 677 (1964).

[8] Grondin, R.O., Blakey, P.A., and East, J.R., "Effects of Transient Carrier Transport in Millimeter Wave GaAs Diodes," *IEEE Trans. Electron Devices*, ED-31, 21 (1984).

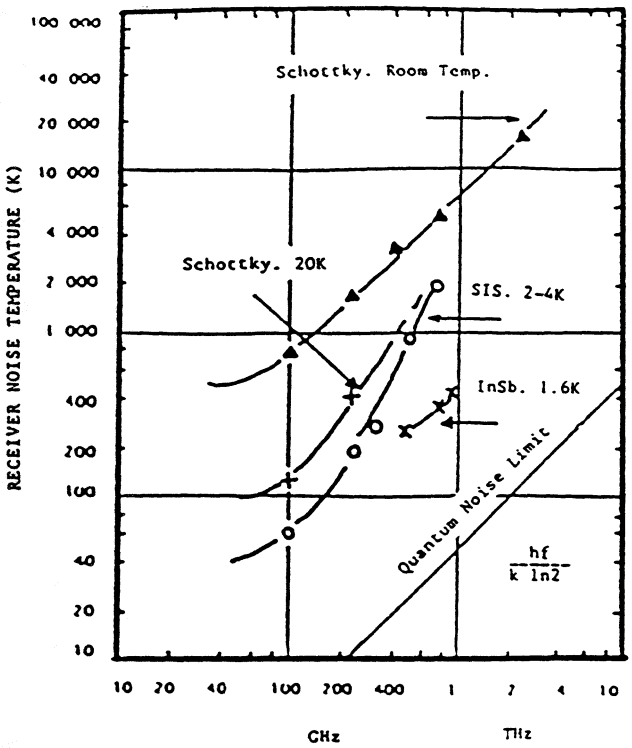

Figure 1. Best noise temperatures achieved for receivers from 100 GHz through 2 THz.

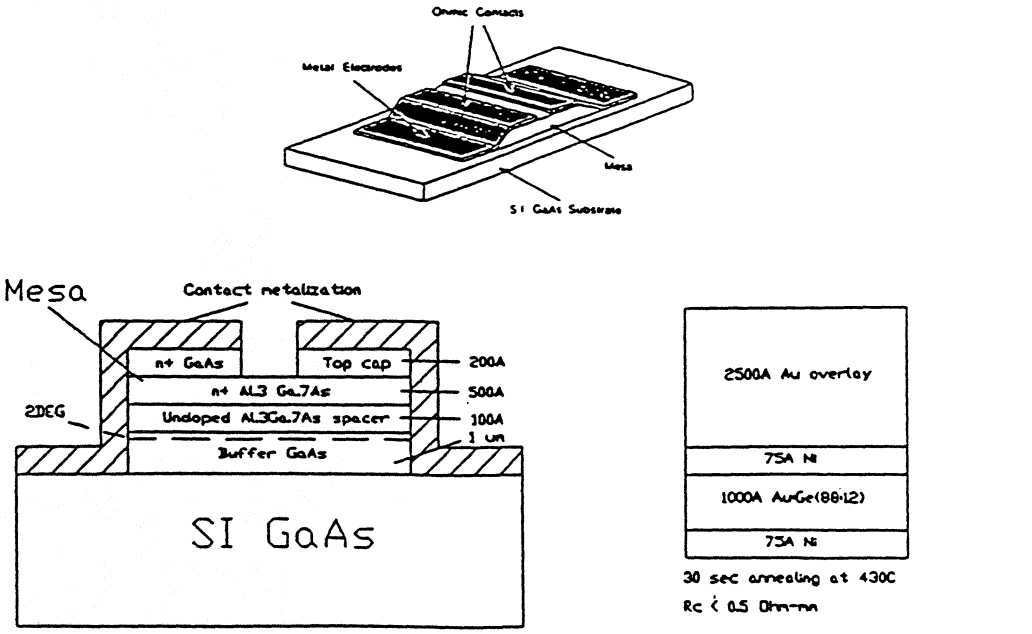

Figure 2. Outline and cross-section of the 2DEG device.

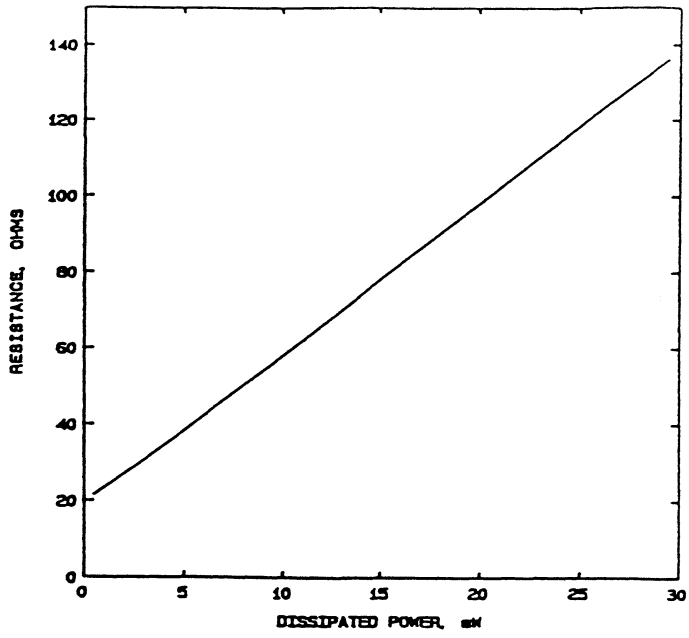

$$C = \frac{dR}{dP} \cong \text{constant}$$

Figure 3. Resistance versus dissipated power for 2DEG device at 77K.

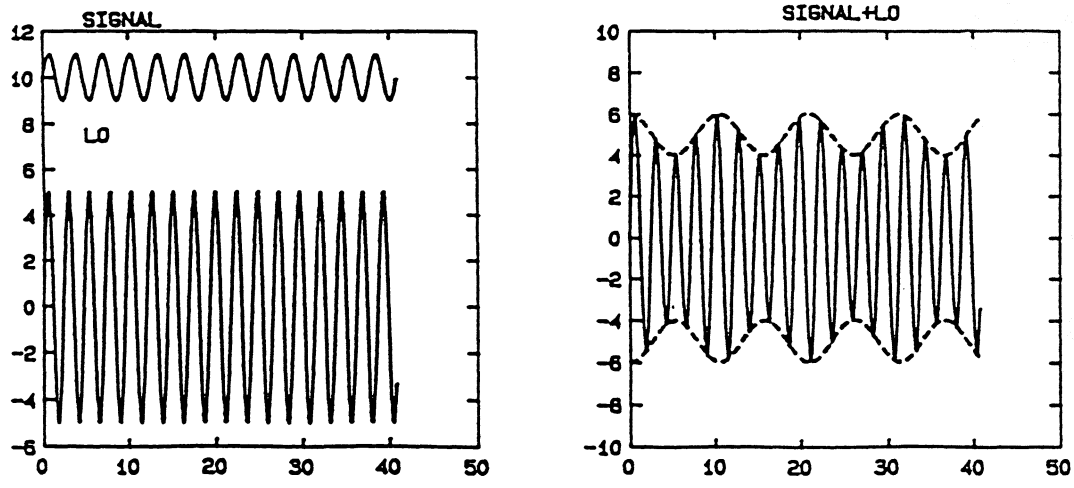

Figure 4. Illustration of the operation of a hot electron mixer.

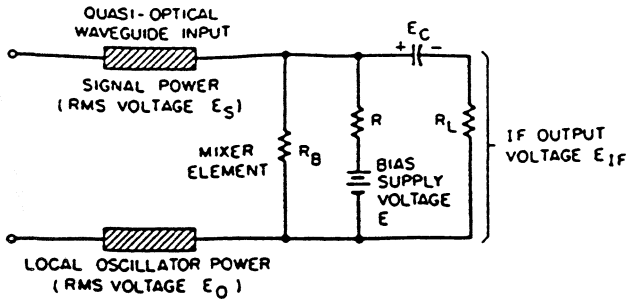

Figure 5. Equivalent circuit of hot electron mixer device.

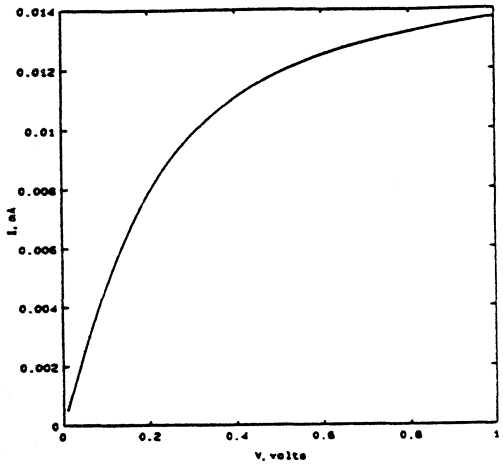

Figure 6. I–V–curve for 2DEG device at 77K.

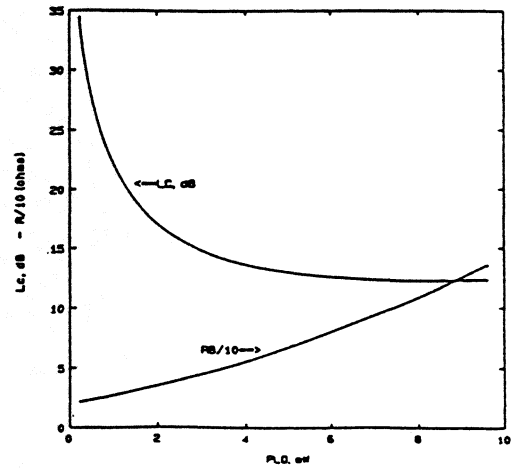

Figure 7. Calculated conversion loss of 2DEG mixer, based on I–V–curve of Figure 6.

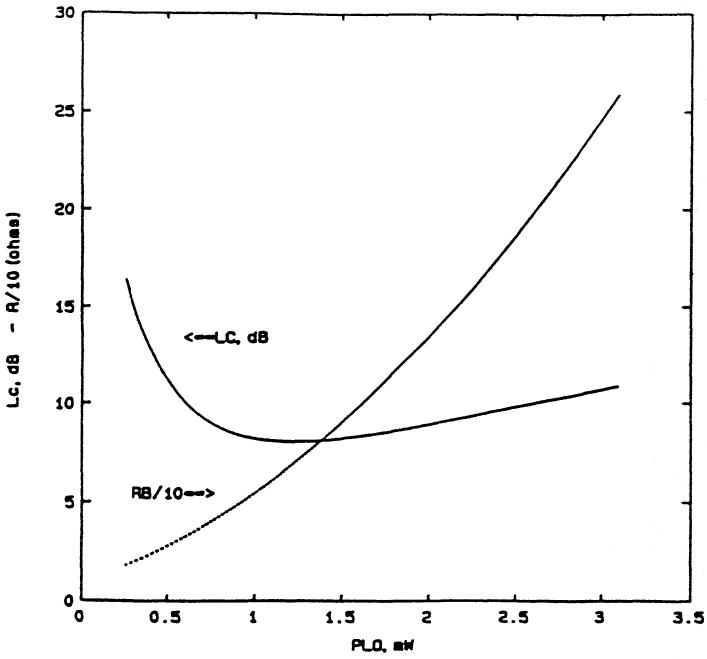

Figure 8. Calculated conversion loss for 2DEG device at 77K, based on improved I–V–curve.

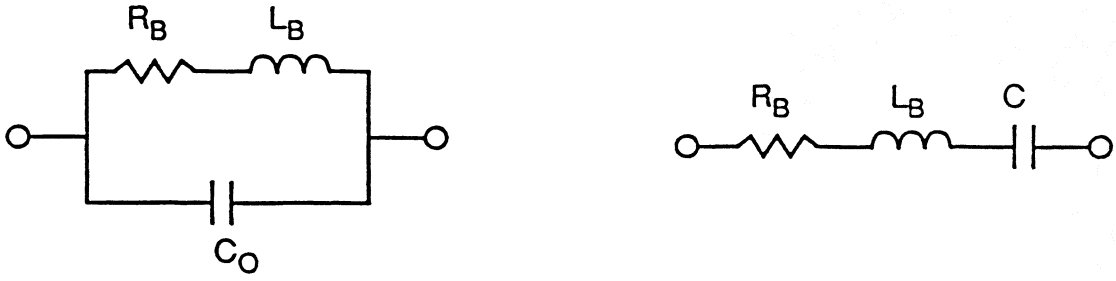

Figure 9. a) Equivalent circuit of 2DEG devices, with parasitics. b) Inductance of device is tuned out with series capacitance.

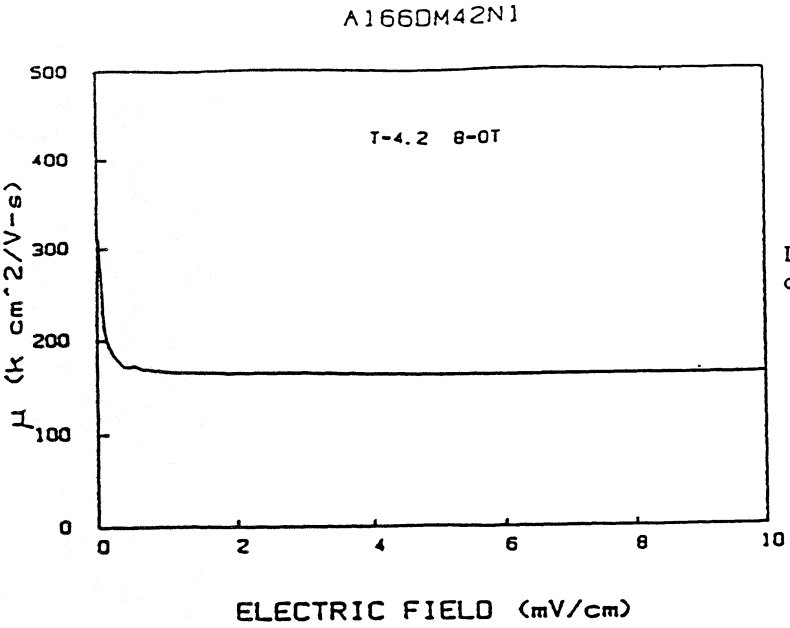

Low field drift mobility of the 2-DEG.

Figure 10.

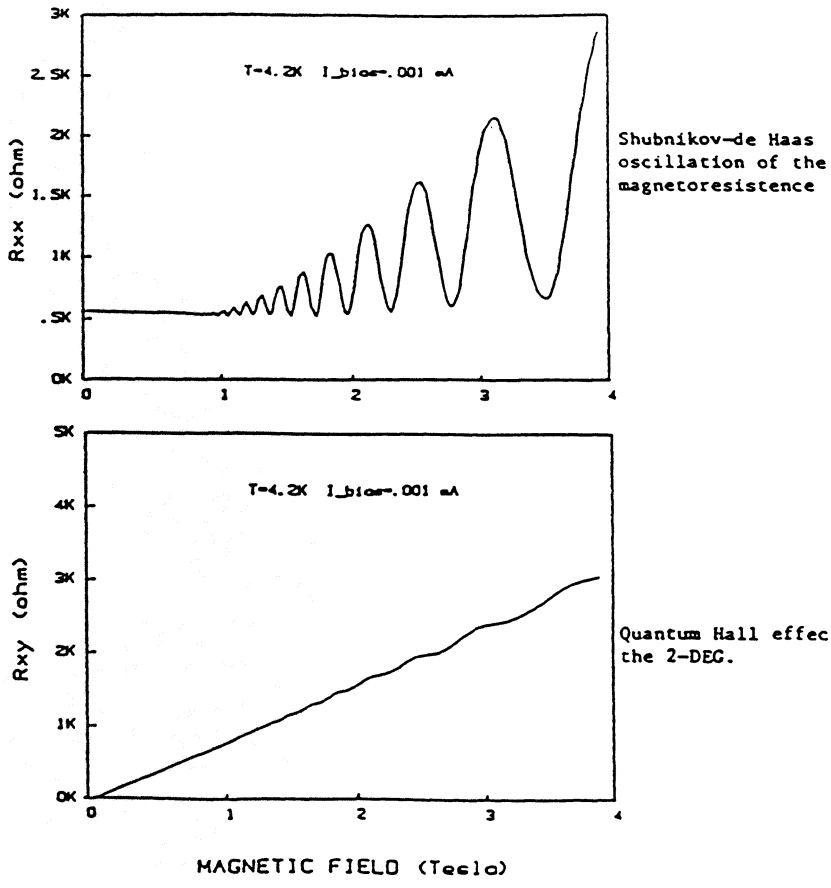

Shubnikov-de Haas oscillation of the magnetoresistence

Quantum Hall effect of the 2-DEG.

Figure 11.

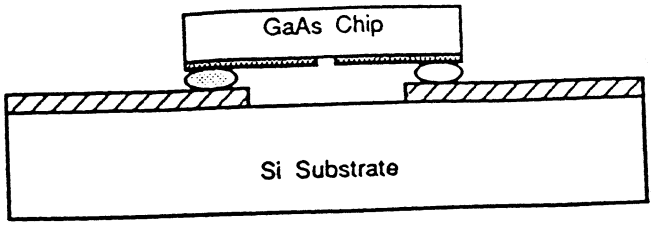

Figure 12. Flip-chip mounting of the device across slot-line circuit.

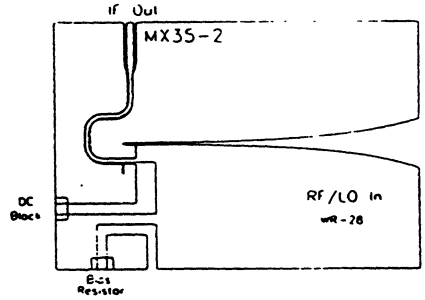

(a) Full view

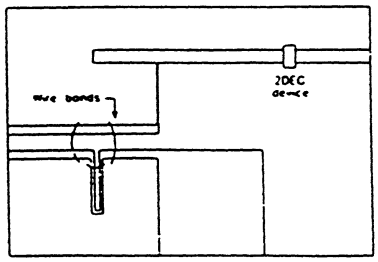

(b) Detailed view of transition, matching stub

Figure 13. Circuit for 35 GHz mixer.

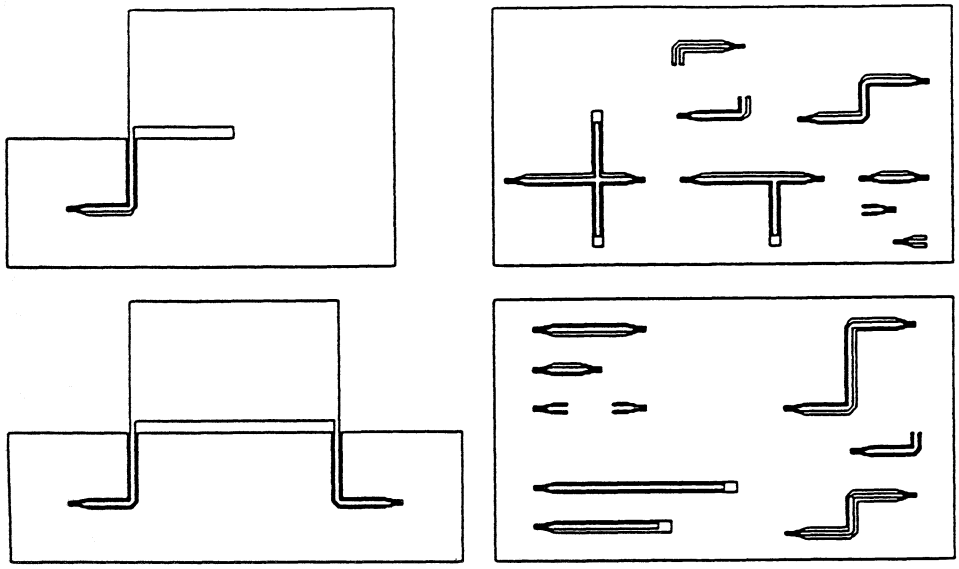

Figure 14. Test chip for microprobing of uniplanar circuit elements.

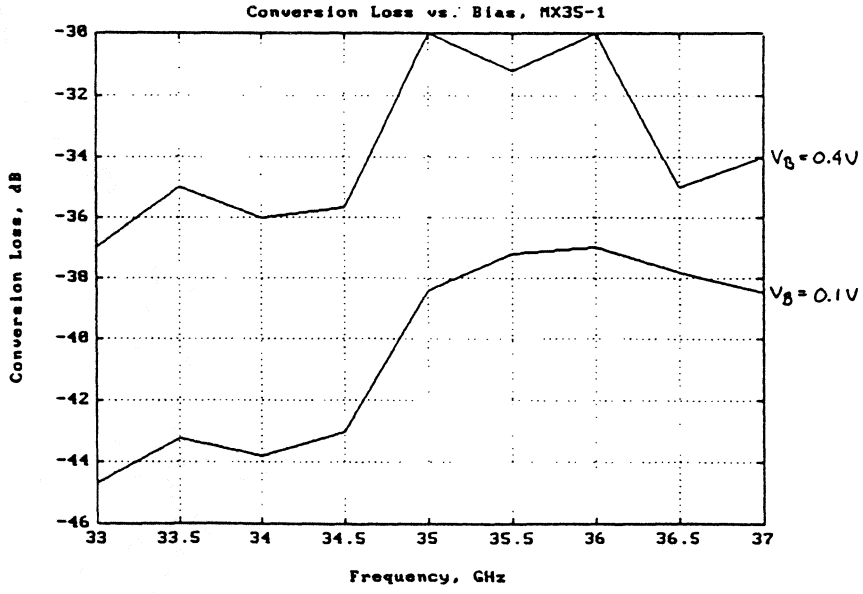

Figure 15. Measured conversion loss of 35 GHz 2DEG mixer at 77K.